Cell Biochem Biophys (2012) 62:125–135
DOI 10.1007/s12013-011-9270-9

ORIGINAL PAPER

Interference of IP-10 Expression Inhibits Vascular Smooth Muscle Cell Proliferation and Intimal Hyperplasia in Carotid Artery: A New Insight in the Prevention of Restenosis

Hu Zuojun · Hu Lingyu · He Wei · Yin Henghui · Zhang Chonggang · Wang Jingsong · Wang Mian · Liu Yong · Wang Shenming

Published online: 18 August 2011

Abstract After vascular angioplasty, vascular smooth muscle cell (VSMC) proliferation causes atherosclerosis and intimal hyperplasia leading to restenosis. Interferon-γ-inducible protein (IP)-10 plays a role in atherogenesis, but the mechanism remains unclear. We evaluated the role of IP-10 in intimal hyperplasia and restenosis. IP-10 expression was determined in arterial specimens from 20 arteriosclerotic obliteration patients and 6 healthy individuals. VSMCs were stimulated in vitro with IFN-γ and transfected with IP-10 siRNA. Silencing was verified with RT-PCR/Western blot; cell proliferation rate was detected by methyl-thiazol-tetrazolium. The carotid artery model of atherosclerosis injury was established with IP-10 siRNA. IP-10 expression was detected at 1 and 4 weeks using RT-PCR and immunohistochemistry. Artery morphology was assessed with hematoxylin-and-eosin staining, and intimal hyperplasia was evaluated by electron microscopy. IP-10 was overexpressed in arteriosclerotic obliteration group compared with control group ($P < 0.05$). IP-10 expression in transfected group was significantly lower than in untransfected group. The intima-to-media ratio of transfected group at 4 weeks was lower than that of untransfected group ($P < 0.01$). The transfected group exhibited more regular intimal structure and less hyperplasia under electron microscopy. We, therefore, concluded that IP-10 played an important role in intimal hyperplasia as siRNA-mediated IP-10 silencing inhibited aberrant VSMCs hyperplasia and reduced restenosis.

H. Zuojun (✉) · H. Lingyu · H. Wei · Y. Henghui · Z. Chonggang · W. Jingsong · W. Mian · L. Yong · W. Shenming
Department of Vascular Surgery, First Affiliated Hospital of Sun Yat-sen University, Guangzhou 510080, China
e-mail: zuojunhu@hotmail.com

Keywords IP-10 · Intimal hyperplasia · Smooth muscle cells · siRNA · Restenosis

Introduction

Hyperplasia of the tunica intima causes arteriosclerotic obliteration restenosis after vascular interventional therapy. Although the specific mechanism is unclear, accumulating evidence indicates that the inflammatory response plays an important role in this process [1]. IP-10, a member of the chemokine CXC family, is part of the early phase of inflammatory response under interferon-gamma (IFN-γ) stimulation and was initially discovered in the human U937 lymphoma cells [2]. It is different from other CXC family members in that IP-10 exerts chemotactic effects on monocytes and activates T lymphocytes [3]. Several studies have investigated the role of IP-10 in inflammatory response and immune reactions. IP-10, as a secretary factor in early phase, determined the severity of host reaction in pulmonary disease [4]. In addition, IP-10 also played an important role in the primary immune responses of SARS [5], hepatitis [6], and tuberculosis [7]. The overexpression of IP-10 was also documented in diabetes mellitus [8–10] and autoimmune thyroid diseases [11–13]. Studies on the role of IP-10 in transplantation immunity found that IP-10 could not only attract monocytes and activate T lymphocytes but it also affected biological properties of the vascular wall [14]. IP-10 has effects on both immune cells and vascular cells, indicating its important role in chronic rejection characterized by immune-induced vascular smooth muscle cell (VSMC) proliferation and graft angiosclerosis. Following heart transplantation, IP-10 increases directly associated with chronic rejection reaction [15]; IP-10

recruited T cells to the heart which in turn altered the functions of vascular endothelial cells and smooth muscle cells [16–19].

As an active factor in the inflammatory response, IP-10 is also involved in atherogenesis and was reported [20] to have potential effects on VSMC proliferation and migration. During the formation of atherosclerosis, IP-10 overexpression in vascular cells plays an important role in T cell activation and colonization. IP-10 was found to be highly expressed in endothelial cells, smooth muscle cells, and macrophages of the atheromatous plaque [21].

Nevertheless, the role of IP-10 in the VSMC proliferation remains to be elucidated. VSMC proliferation, as the pathological basis of atherosclerosis and intimal hyperplasia after vascular injury [22, 23], can cause vascular stenosis and compromise the clinical outcome of this disease [24, 25]. Although the chemotactic and activating effects of IP-10 on T cells and monocytes during inflammatory response have been demonstrated, its direct effects on the vascular wall cells and relevant mechanisms remain unclear. In this regard, we hypothesized that IP-10 directly stimulates the VSMC proliferation, and the inhibition of IP-10 expression can suppress the aberrant VSMC proliferation and overproliferation of vascular intima. In this article, we demonstrate by using in vivo and ex vivo study models that IP-10 plays an important role in the intimal hyperplasia as the siRNA-mediated IP-10 silencing inhibits aberrant VSMCs hyperplasia and reduces restenosis after vascular injury.

Materials and Methods

Patients and Experimental Design

The study was approved by the ethics committee of our hospital, and written informed consent was obtained from all the patients and healthy controls. Artery specimens were obtained from 20 patients (14 males and 6 females, aged from 55 to 78 years) with arteriosclerotic obliteration that underwent amputation and 6 healthy individuals (4 males and 2 females, aged from 32 to 67 years) who were involved in fatal accidents and had kindly donated samples and organs before death. An immunohistochemical assay was employed to determine changes in the expression of IP-10 in vascular wall. A small interference RNA (siRNA) eukaryotic expression plasmid for IP-10 was established. For in vitro experiments, the IP-10 siRNA was transfected into primary VSMC culture, and the changes in IP-10 expression and VSMC proliferation in response to exogenous stimulation were observed. Finally, the carotid artery model of atherosclerosis injury was introduced; IP-10 siRNA was transfected locally to determine changes in vascular intima and evaluate the role of IP-10 in vascular intimal hyperplasia.

Experimental Animals and Reagents

New Zealand rabbits were purchased from Guangzhou University of Chinese Medicine (SYXK Yue 2007-0081). Mouse anti-human IP-10 antibody was purchased from Abcam (8098; Cambridge, UK); GAPDH monoclonal antibody (mAb) and secondary antibody were purchased from Santa Cruz Company (CA, USA); IP-10 siRNA expression plasmid was purchased from Shanghai GeneChem Co., Ltd (Shanghai, China); Lipofectamine 2000 transfection reagent and Trizol were from Invitrogen (CA, USA); Reverse transcription kit (FSK-100) was from Toyobo company (Osaka, Japan); PCR kit (DRR019A) was from Takara (Shiga, Japan); IP-10 primers were from Invitrogen (CA, USA). DMEM cell culture medium and fetal calf serum (FCS) were purchased from Gibco (Paisley, UK); and VSMC primary cultures were prepared in our laboratory, and generations of 5-10 were used in the experiments.

IP-10 Expression in Human Vascular Wall

The artery specimens from 20 patients and six healthy individuals were treated with IP-10 mAb as the primary antibody following the manufacturer's instructions. The chromogenic development reagent, 3,3′ diaminobenzidine (DAB) was used for visualization with hematoxylin counterstaining. The specimens were observed under light microscopy at $\times 200$ magnification. Positive IP-10 staining was defined as brown–yellow or brown granules within the smooth muscle cell plasma or membrane.

Construction of IP-10 siRNA Eukaryotic Expression Plasmid

We retrieved the IP-10 gene sequence from GeneBank and searched for siRNA sequences using the Ambion siRNA target finder server (www.ambion.com/techlib/misc/siRNA-finder.html). The sequence with the highest score was used as IP-10 gene interference sequence: 5′-GAC CAA TGA TGG TCA CCA AAT TTC AAG AGA ATT TGG TGA CCA TCA TTG GTC-3′. The polyclonal restriction sites of the eukaryotic expression plasmid pGCsilencer-U6 were digested with restriction endonucleases *Bam*H1 and *Hin*dIII. The IP-10 target segment and linearized plasmid were joined by T4DNA ligase to construct the plasmid pGCsilencer-U6-IP-10-siRNA.

Separation, Culture, and Identification of VSMC

The adventitia of femoral arteries from the healthy individuals was stripped off using tissue-explant method described previously [26], followed by removal of intima. The vessels were cut into tissue blocks (1-mm diameter)

and transferred to culture flask. After incubation in the bottom of flask for 6 h with DMEM containing 20% FCS at 37°C (5% CO_2), the flask was turned over and incubated for static culture. The medium was changed every 3 days. Primary cells were subcultured at confluence for three generations. The immunohistochemical assay using mouse anti-human smooth muscle α-actin mAb was performed on cells attached to cover slips.

Transfection of IP-10 siRNA

The VSMC primary cultures (generations 5–10) were divided into negative control, blank plasmid control, and siRNA interference groups. Each well of the 6-well plate was seeded with 2×10^5 cells. At 40–50% confluency, transfection reagent was added to the cell culture media. Six hours later, the medium was replaced with DMEM medium containing 10% FCS and cells were incubated for 24 h. After observing green fluorescence, cell culture medium was replaced with serum-free medium; IFN-γ (100 ng/ml) was added after 48 h. The following solutions were prepared for transfection. For interference group, 4 μg of siRNA plasmid and 250 μl of serum-free medium were mixed for 5 min, while 5 μl of Lipofectamine 2000 and 250 μl of serum-free medium were mixed separately and also kept for 5 min. Subsequently, the two mixtures were combined and allowed to stand at room temperature (RT) for 20 min. For blank plasmid group, 4 μg of blank plasmid and 250 μl of serum-free medium were mixed by gentle swirling and kept for 5 min, while 5 μl of Lipofectamine 2000 and 250 μl of serum-free medium were also mixed and kept for 5 min. Then, the two mixtures were combined and allowed to stand at RT for 20 min. For negative control group, 2 ml of serum-free medium was used.

Detection of IP-10 mRNA by RT-PCR

After stimulation with IFN-γ for 24 h, 0.5 ml of Trizol was added to each well, and total RNA was extracted according to the manufacturer's instructions. Reverse transcription was carried out with oligo-dT primers, and then the target sequence was amplified using PCR. Primer sequences were as follows: IP-10 forward, 5′-CCT CCA GTC TCA GCA CCA TGA ATC-3′, IP-10 reverse, 5′-GAT GCA GGT ACA GCG TAC AGT TCT A-3′, (116 bp product); β-actin forward, 5′-CCA TGT ACG TAG CCA TCC A-3′, β-actin reverse, 5′-GAT AGA TCC ACC AAT CCA C-3′, (515 bp product).

Thermal cycling conditions were as follows: denaturation at 94°C for 5 min followed by 30 cycles of 94°C for 30 s → 60°C for 30 s → 72°C for 60 s and final extension at 72°C for 5 min. PCR products were separated on 2% agarose gel and photographed for analysis.

Detection of IP-10 Protein Expression in Smooth Muscle Cells by Western Blot

Proteins were extracted after 24 h of the treatment and quantified by Coomassie brilliant blue. Proteins were separated using 12% SDS-PAGE gels loaded with 50 μg of protein sample per lane. After gel electrophoresis, samples were transferred to nitrocellulose membrane, blocked with non-fat milk, and then incubated with IP-10 mAb (1:20 dilution) for 16 h at 4°C. The samples were rewarmed for 1 h, washed thrice with PBST (phosphate buffered saline containing 0.1% Tween-20), 10 min each wash. Membranes were then incubated with secondary antibody (1:4000 dilution) for 2 h, washed thrice with PBST as before, followed by development and result analysis using enhanced chemiluminescence detection method according to the manufacturer's recommendations (Amersham Biosciences, Arlington Heights, Boston, USA), and subsequent exposure of the membranes to film.

Detection of Smooth Muscle Cell Proliferation by MTT Assay

Cells were seeded into the 96-well plate (2×10^3 per well) in DMEM culture medium containing 10% FBS and were incubated at 37°C in 5% CO_2. After the adherence of cells to wells, medium was replaced with serum-free medium, and cells were incubated for 24 h. Transfection solutions were prepared and added as described before. After 48 h, IFN-γ (100 ng/ml) was added. Methyl-thiazol-tetrazolium (MTT; 5 mg/ml) was added (20 μl/well) at the intervals of 24, 48, 72, 96, and 120 h after the addition of IFN-γ. After an additional incubation of 4 h, culture medium was carefully removed from the wells, and dimethyl sulfoxide (DMSO; 150 μl per well) was added. The plates were agitated at RT in dark for 10 min, and then absorbance was measured at the wave length of 570 nm.

Carotid Artery Animal Model Construction and Transfection

A total of 30 male New Zealand rabbits (weighing 2.0–2.5 kg) were purchased from Guangzhou University of Chinese Medicine (license, SYXK Yue 2007-0081). The rabbits were randomly and equally divided into negative control, blank, and interference groups. Animals were fed on a high-fat diet containing 1% cholesterol and 0.5% lard for 8 weeks to establish the atherosclerotic injury carotid artery model as described previously [27]. *Preparation of siRNA:* siRNA (50 μg) was diluted in 200 μl of physiological saline, and 150 μl of cationic liposome Lipofectamine 2000 was dissolved in 250 μl of normal saline; then, the two solutions were mixed and stored at RT for

10–15 min. The rabbit was anesthetized by intravenous administration of 3% pentobarbital sodium (30 mg/kg) and heparin (200 U/kg) via the ear vein. The rabbit was immobilized in a recumbent position, hair of the neck was removed, and the skin was disinfected and draped. An incision was made in the midline of the neck, and the left carotid artery (6 cm) was exposed and separated; then, internal and external carotid arteries were separated. Proximal ends of the common and internal carotid arteries were clipped, the distal end of the external carotid artery was ligated, and the proximal end was lifted with line. A V-shaped excision was made on the external carotid artery 0.5 cm away from the bifurcation of external and internal carotid arteries. The 4F Fogarty balloon catheter was inserted retrogradely, heparin saline was injected into the balloon to 202.6 kPa, and then the catheter was drawn back from the proximal end. The process was repeated three times, and the catheter was removed. A 3F Fogarty catheter with a tip punctured with a syringe was introduced into the artery, and transfection solution was injected as follows: (i) experimental group, IP-10-siRNA/Lipofectamine 2000; (ii) blank plasmid group, blank plasmid/Lipofectamine 2000; and (iii) negative control group, physiological saline. The solution was retained for 30 min. The catheter was then removed, and the proximal end of external artery was ligated. The artery clipper was opened to restore the carotid artery blood flow, wound was flushed with physiological saline, and the incision was sutured. Penicillin (800,000 U) was injected once daily (intramuscularly in the leg) for 3 days after the procedure.

Half of the rabbits in each group were sacrificed for carotid artery specimens at each time point (1 and 4 weeks post surgery). One subject in the blank plasmid group died after surgery. Specimens were stained with H&E staining and immunohistochemical staining using anti-IP-10 mAb and subsequently fixed for electron microscopy. The remaining specimens were preserved at −80°C for RT-PCR analysis.

IP-10 mRNA Detection by RT-PCR in the Animal Specimens

Total RNA was extracted from 100 mg of tissue sample using Trizol according to the manufacturer's instructions. Reverse-transcription with oligo-dT primers produced cDNA for PCR amplification. The primer sequences were as follows: IP-10 forward, 5′-CCT CCA GTC TCA GCA CCA TGA ATC-3′, IP-10 reverse, 5′-GAT GCA GGT ACA GCG TAC AGT TCT A-3′, (116 bp product); β-actin forward, 5′-CCA TGT ACG TAG CCA TCC A-3′, β-actin reverse, 5′-GAT AGA TCC ACC AAT CCA C-3′, (515 bp product). Thermal cycling conditions were as follows: denaturation at 94°C for 5 min followed by 30 cycles of 94°C for 30 s → 60°C for 30 s → 72°C for 60 s and final extension at 72°C for 5 min. Then, 2% agarose gel electrophoresis was performed, and the gel was photographed for analysis.

Immunohistochemical Staining of Animal Specimens

Staining was performed using the primary IP-10 mAb according to the manufacturer's instructions. Slices were stained following the manufacturer's instructions for the corresponding reagents, developed with DAB, and counterstained with hematoxylin. The host vessels harvested along with the graft were allowed to react with phosphate-buffered saline (PBS) in place of the primary antibodies and served as positive control. Specimens were examined and photographed under light microscopy (magnification ×200). Positive IP-10 staining was defined as brown–yellow or brown granules within the smooth muscle cell plasma or membrane.

Histopathological Examination of Animal Specimens

Histopathological examination of the carotid artery specimens (H&E-stained) was performed and photographed (magnification ×200) according to the previously published protocol [28]. Also, the intima-to-media (I:M) ratio was measured.

Transmission Electron Microscopy of Vascular Specimens

The samples were fixed with 2.5% glutaraldehyde for 24 h and then washed with PBS overnight. Next day, the specimens were washed six times with PBS, 20 min each wash; dehydrated twice by ethanol using the sequential concentrations of 30, 50, 70, and 90% (15 min each). Then, the samples were dehydrated thrice by anhydrous alcohol, 15 min each treatment, and soaked twice in tert-butanol, 15 min each time. The specimens were dried under vacuum (4°C) for 3 h. The dried specimens were adhered to the metal table and sprayed with gold, and the intimal growth of the artery was observed by transmission electron microscope.

Statistical Analysis

Quantitative data were expressed as mean ± SD values. Analysis was performed using SPSS 16.0 (SPSS Inc, Chicago, IL, USA) statistical software. Multi-group comparisons were performed with one-way ANOVA. Enumeration data were tested with exact probability test. The differences were considered significant at P-values of <0.05.

Results

IP-10 Expression in the Human Vascular Wall

Immunohistochemical staining demonstrated IP-10 overexpression in the vascular wall samples from the 20 cases with arteriosclerotic obliteration, while only one case from the healthy control group showed IP-10 overexpression (Fig. 1; $P < 0.05$). The results indicate that IP-10 plays an important role in the pathogenesis of arteriosclerotic obliteration.

IP-10 mRNA Expression in VSMCs

First, with regard to the construction and identification of IP-10 siRNA eukaryotic expression plasmid, the inserted target sequence was identified to be consistent with the designed interference target sequence by enzyme digestion and sequencing. The siRNA insert was verified by sequencing (data not shown) and inserted into the expression vector pGCsilencer^{TM}-U6 to construct the IP-10 siRNA eukaryotic expression plasmid. VSMCs were identified by α-actin immunocytochemical staining; the cytoplasm appeared yellow brown at microscopic examination (Fig. 2), which was the expected positive result (cultured cells were VSMC) while the negative controls (without adding first antibody) did not show staining. IP-10 mRNA expression was significantly lower in interference group as compared with blank control groups (Fig. 3).

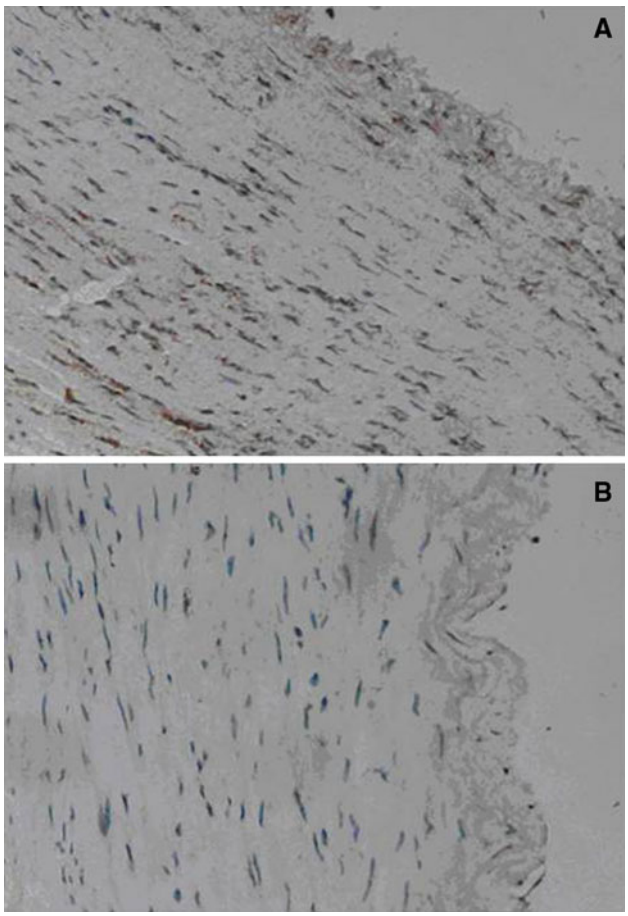

Fig. 1 IP-10 immunohistochemical staining of human femoral artery (×200; Diaminobenzidine staining). **a** Arteriosclerotic obliteration group; **b** healthy controls

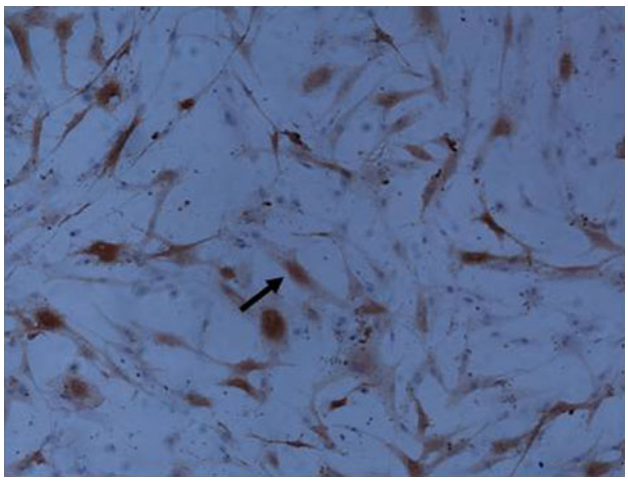

Fig. 2 Immunohistochemical staining of vascular smooth muscle cells (VSMCs; ×100). VSMCs were identified by immunocytochemical staining for α-actin; the cytoplasm appeared *yellow brown* (*arrow*) which was the expected positive result for VSMC while the negative controls (without adding primary antibody) did not show staining (Color figure online)

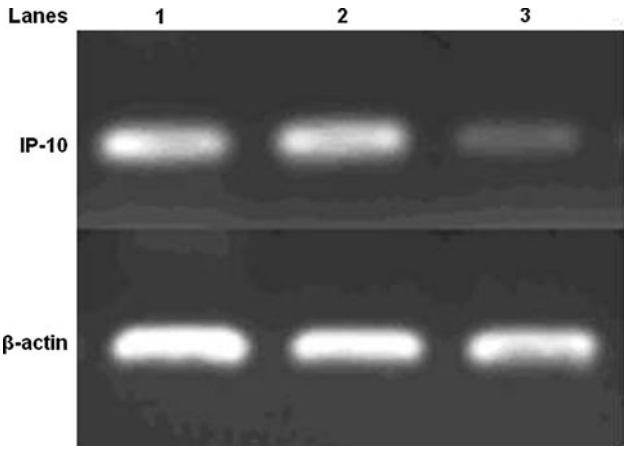

Fig. 3 RT-PCR showing IP-10 mRNA expression in VSMCs. Total cellular RNA was extracted using Trizol method followed by reverse transcription and PCR amplification for interferon-γ-induced protein (IP-) 10 as described in "Materials and Methods" section. In agarose gel, *lanes 1, 2*, and *3* represent negative control, blank control and interference groups, respectively. IP-10 mRNA expression was significantly lower in interference group as compared with blank control groups

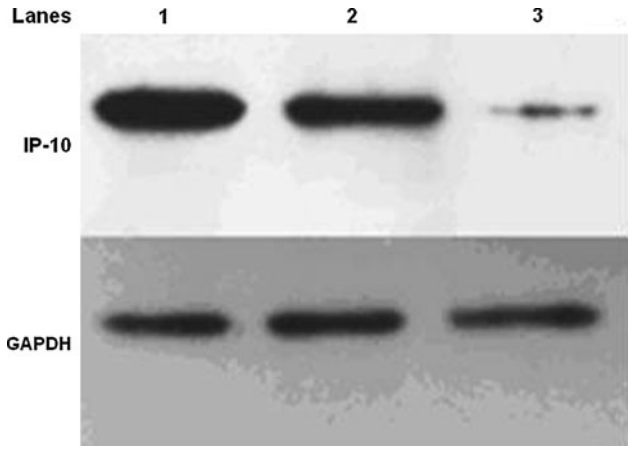

Fig. 4 Western blot showing IP-10 protein expression in VSMCs. Expression of IP-10 protein was determined using SDS-PAGE as described in "Materials and Methods" section. In polyacrylamide gel, *lanes 1, 2*, and *3* represent negative control, blank control, and interference groups, respectively. IP-10 protein expression in interference group reduced significantly after IP-10 siRNA transfection, while the expression in negative control and blank plasmid groups remained unchanged

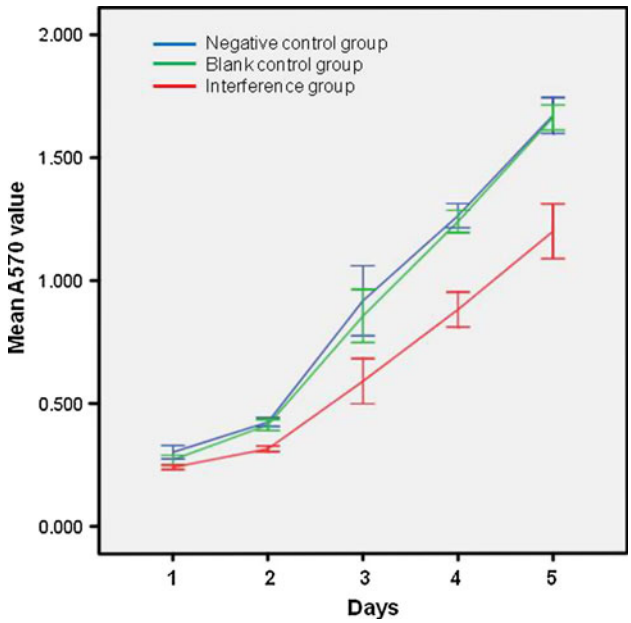

Fig. 5 Growth detection in VSMCs by MTT proliferation assay. Cells (2×10^3 per well) were cultured (DMEM with a0% FBS) in 96-well plate (2×10^3 per well). After adherence, cells were cultured in serum-free medium for 24 h. IP-10 siRNA transfection solutions were prepared and added as described in "Materials and Methods" section. After 48 h, IFN-γ was added (100 ng/ml). MTT (5 mg/ml) was added (20 μl/well) at the intervals of 24, 48, 72, 96, and 120 h after the addition of IFN-γ. After an additional incubation of 4 h, culture medium was removed and dimethyl sulfoxide (DMSO) was added (150 μl/well). The plates were agitated at room temperature in the dark for 10 min, and the absorbance was measured at 570-nm wave length. After IP-10 siRNA transfection, absorbance in the transfected group at each time point was significantly lower than that in negative control and blank groups. *Error bars* show ± 1SD

IP-10 Protein Expression in VSMCs

As shown in Fig. 4, IP-10 protein expression in interference group decreased significantly after IP-10 siRNA transfection, while the expression in negative control and blank plasmid groups remained unchanged.

Effect of IP-10 on VSMC Proliferation

After IP-10 siRNA transfection, absorbance at 570 nm in the transfected group at each time point was significantly lower than that in negative control and blank groups (Fig. 5).

IP-10 mRNA Expression in Samples from Atherosclerotic Intimal Injury Model

As shown in Fig. 6, IP-10 mRNA expression in the interference group was significantly lower than that in negative and blank groups at week 1 ($P < 0.01$) and week 4 ($P < 0.05$).

IP-10 Protein Expression in the Rabbit Model (Immunohistochemistry)

Immunohistochemical staining of the carotid artery sections showed that vascular endothelium and VSMC were

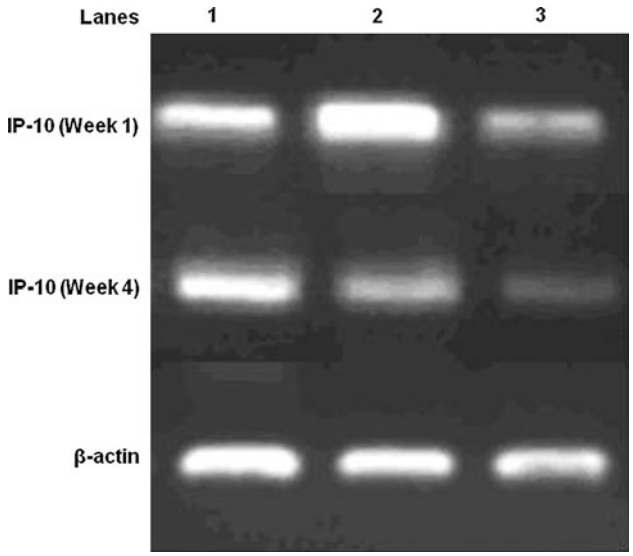

Fig. 6 RT-PCR of IP-10 mRNA expression in the rabbit model. The mRNA expression of IP-10 was measured by RT-PCR at weeks 1 and 4 of atherosclerotic intimal injury in the vascular samples from the rabbit model, following the procedure as described in "Materials and Methods" section. In agarose gel, *lanes 1, 2*, and *3* represent negative control, blank control, and interference groups, respectively. IP-10 mRNA expression in interference group was significantly lower than that in negative and blank groups at both week 1 ($P < 0.01$) and week 4 ($P < 0.05$)

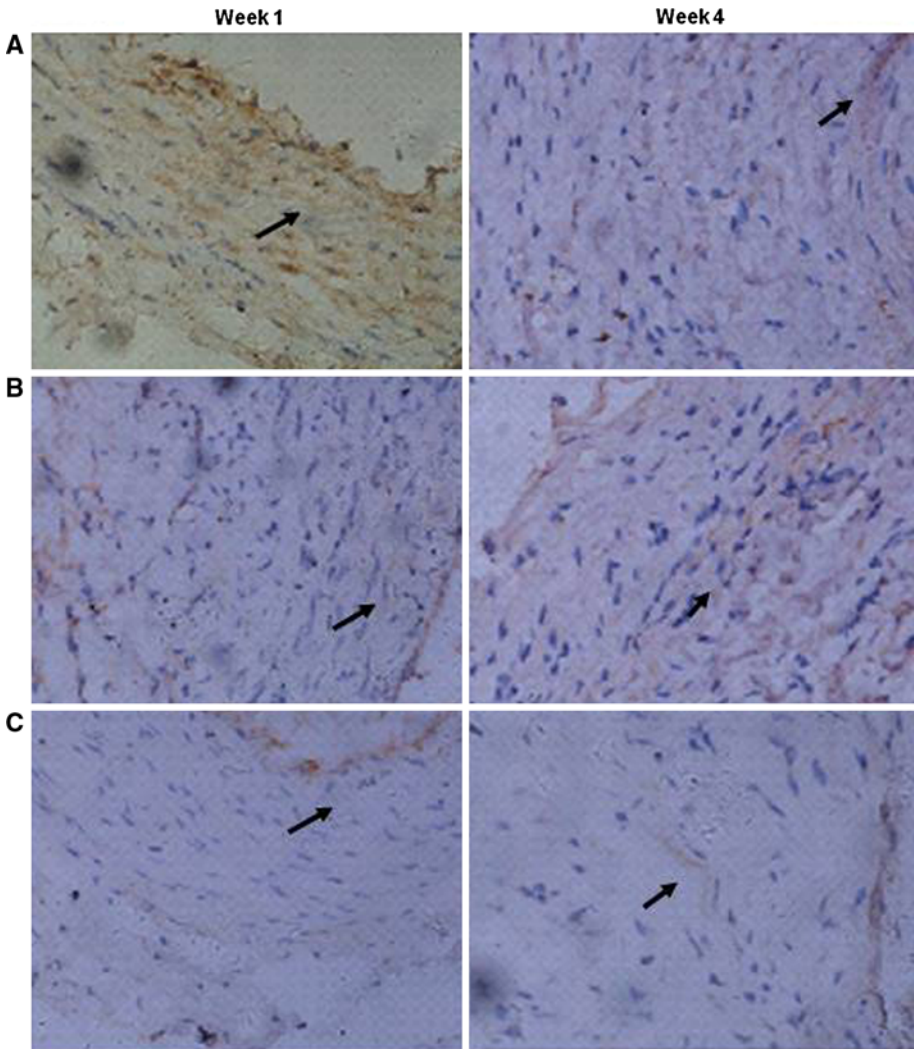

Fig. 7 IP-10 Immunohistochemical staining in carotid artery (×400, Diaminobenzidine staining). The carotid artery samples were stained to determine IP-10 expression at weeks 1 and 4 using DAB staining as described in "Materials and Methods" section. Positive IP-10 staining was defined as *brown–yellow* or *brown* granules (*arrows*) within the smooth muscle cell plasma or membrane. **a** Negative control group; **b** blank control group; **c** interference group (Color figure online)

negative for IP-10 in the normal carotid artery at 1 week (Fig. 7); in contrast, VSMCs and vascular endothelial cells were weakly positive in interference group and strongly positive in negative and blank plasmid groups. At 4 weeks, the VSMC and vascular endothelial cells were positive in all the groups with non-significant differences observed.

H&E Staining of Carotid Artery and the Intima-to-Media Ratio

H&E-stained carotid artery sections showed marked stenosis in negative and blank plasmid control groups. In both the negative and blank plasmid control groups, at week 1 postoperatively, the artery structure was disrupted and the endothelium and internal elastic laminae were fragmented. After week 4, the intima had thickened considerably, and the smooth muscle cells of the tunica media were irregularly arranged, with the VSMCs penetrating through the internal elastic lamina to the endothelium. While being in interference group, a few endothelial cells had broken off at week 1, the internal elastic laminae were separated and fragmented, and the thickening of intima was not significantly different from controls. However, at week 4, the intimal thickening in interference group was considerably reduced as compared with negative and blank plasmid control groups (Fig. 8). In addition, the intima-to-media ratio was significantly different between interference and control groups (Table 1).

Electron Microscopy of the Carotid Artery Specimens

At week 1 after the surgery, electron microscopy revealed that the intimal structure was irregular, the internal elastic lamina was fragmented, and the intima had begun to repair (Fig. 9). There was no significant difference observed among negative and blank plasmid control groups, and

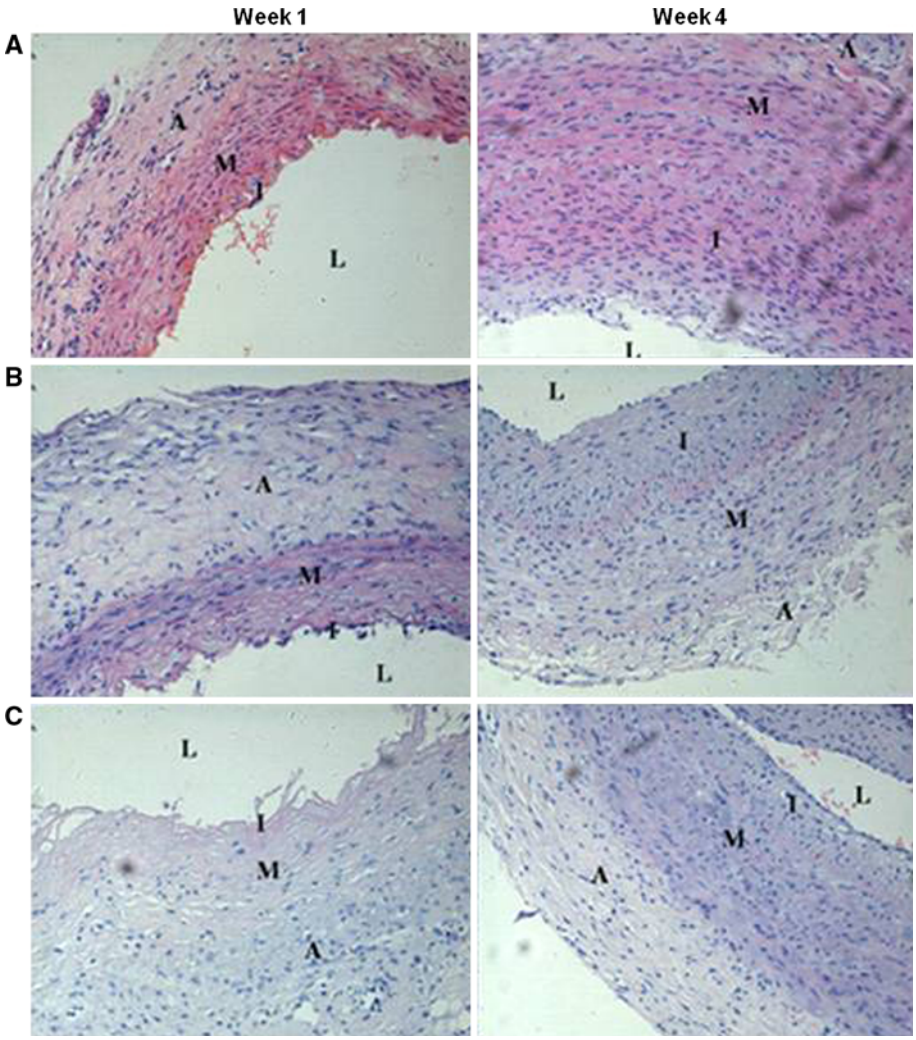

Fig. 8 H&E staining of carotid artery specimens (×200). H&E staining revealed marked stenosis in negative (**a**) and blank plasmid (**b**) control groups as compared with interference group (**c**). In both negative and blank plasmid control groups, at week 1 postoperatively, the artery structure was disrupted and the endothelium and internal elastic laminae were fragmented. At week 4, the intima had thickened considerably, and the smooth muscle cells of the tunica media were irregularly arranged, with the VSMCs penetrating through the internal elastic lamina to the endothelium. While being in interference group, a few endothelial cells had broken off at week 1, the internal elastic laminae were separated and fragmented, and thickening of intima was not significantly different from controls. However, at week 4, the intimal thickening in interference group was considerably reduced as compared with negative and blank plasmid control groups

Table 1 Intima-to-media ratio after intimal balloon injury

Parameter	Negative control group	Blank control group	Interference group
Intimal thickness (μm)	218 ± 13.3	210 ± 20.6	109 ± 11.6*
Media thickness (μm)	213 ± 7.4	204 ± 8.6	201 ± 12.1
Intima to media (I:M) ratio	1.02 ± 0.05	1.03 ± 0.07	0.54 ± 0.04*

* *P*-value of <0.01 as compared with other groups

interference groups. However, at week 4 after the surgery, the interference group showed more regular and smooth structures and less intimal proliferation as compared with negative and blank plasmid control groups.

Discussion

A large number of vascular diseases can now be cured because of the growing availability of effective vascular interventional therapy. Nonetheless, vascular restenosis after vascular angioplasty remains a major complication that compromises the longterm clinical outcomes. The pathogenesis of restenosis is unclear. Restenosis is considered a complex process of injury and excessive repair, presenting as a slow progressive restenosis of the vessel(s) involved. The initiation and development of restenosis is influenced by multiple factors including nature of the disease, coexisting disorders and genetic propensity [29]. Besides, early-phase elastic retraction of the vessel, platelet aggregation, mural thrombosis, inflammatory response, VSMC proliferation, extracellular matrix (ECM)

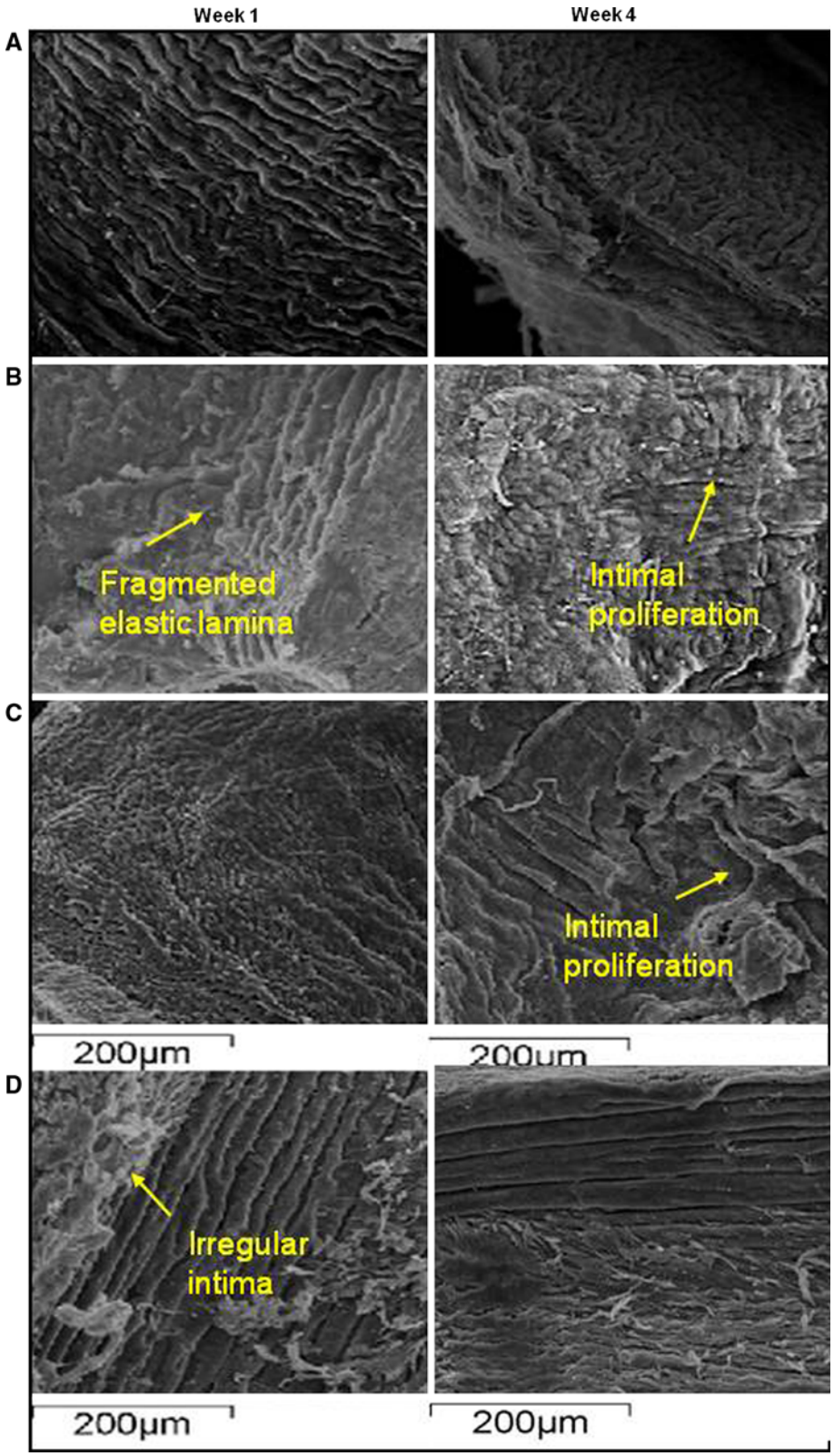

Fig. 9 Electron microphotograph of carotid artery intimal repair. At week 1 after the surgery, electron microscopy revealed that the intimal structure was irregular, the internal elastic lamina was fragmented, and the intima had begun to repair. Compared against normal vessels (**a**), there was no significant difference observed among negative control (**b**), blank plasmid control (**c**), and interference (**d**) groups. However, at week 4 after the surgery, the interference group showed more regular and smooth structures and less intimal proliferation as compared with negative and blank plasmid control groups

deposition, vascular contraction of the injured site, and geometric shape changes of artery have also been hypothesized to play a role in the initiation and development of restenosis. Vascular replacement and angioplasty can cause intimal laceration, vascular over-expansion, and plaque compression, resulting in platelet

activation and thrombosis. The injury-induced activation of platelets, endothelial cells, and smooth muscle cells can release a variety of growth factors, which in turn are able to mediate VSMC proliferation and migration, vascular endothelial cell, and VSMC secretions, increased ECM, and narrowing of the vascular wall [30–34]. Therefore, developing an effective method to inhibit VSMC proliferation is a hotspot in the field of restenosis prevention research.

Interferon γ-induced IP-10 has been demonstrated to promote the VSMC proliferation and migration in vitro following stimulation by inflammation-promoting factors [20]. IP-10 was found to be overexpressed in the mouse carotid artery after angioplasty [20]. In allograft vascular lesions, IP-10 overexpression promoted the initiation of immune-induced vascular lesions characterized by smooth muscle cell proliferation [17]. In the present study, immunohistochemistry revealed overexpression of IP-10 protein in artery lesions of arteriosclerotic obliteration, while RT-PCR and immunohistochemistry revealed that in both negative and blank plasmid control groups, IP-10 was overexpressed in the rabbit carotid artery model, especially in the VSMCs and endothelial cells. Therefore, we speculate that VSMC proliferation might be controlled by inhibiting IP-10 expression. IP-10 is, thus, likely to become a new target in the prevention of vascular restenosis. RNA interference is an effective gene-silencing technique [35] that uses 21–33 bp siRNA to induce degeneration of mRNAs with homologous sequences and thus knocks out target gene expression directionally, specifically, and efficiently. To this end, our group designed and constructed the siRNA eukaryotic expression plasmid pGCsilencer-U6-IP-10-siRNA employing the RNAi principles. This siRNA eukaryotic expression plasmid was successfully used for exploring the IP-10-mediated mechanism(s) of vascular restenosis such as alterations in smooth muscle cells proliferation and intimal hyperplasia after IP-10 silencing.

IFN-γ is an inducer of IP-10. IFN-γ was shown [36] to inhibit the VSMC proliferation after balloon injury and reduce intimal hyperplasia. In our study, IFN-γ promoted IP-10 secretion by VSMCs which, in turn, induced smooth muscle cell proliferation. After transfection with IP-10 siRNA, effects of IFN-γ stimulation via IP-10 induction were suppressed and, hence, VSMC proliferation was also suppressed. Therefore, this in vitro experiment demonstrated that inhibiting IP-10 expression could effectively block the VSMC aberrant proliferation.

Subsequently, we also carried out an in vivo experiment using the rabbit carotid artery intimal injury model. IP-10 expression at the mRNA and protein levels was decreased with local transfection of siRNA, indicating that RNA interference can effectively inhibit IP-10 gene expression. We used the intima-to-media ratio as an index to evaluate the intimal hyperplasia. Our results showed that the intima-to-media ratio in interference group was significantly reduced as compared to that in control groups. At 4 weeks following the transfection, intimal hyperplasia in the interference group was remarkably reduced, and the intimal repair appeared to be smoother and more organized than in control groups. These findings show that RNA interference is able to downregulate the local vascular expression of IP-10, inhibit the intimal hyperplasia by arresting migration of smooth muscle cells to intima and, thus, prevent the development of vascular restenosis after injury.

However, IP-10 mRNA and protein expression at 4 weeks after the transfection was not significantly different among the three groups, which might be because of the limited duration effect of Lipofectamine 2000. Furthermore, long-term effects of IP-10 on injured intima cannot be fully evaluated in such a short duration. Therefore, further studies will be required to investigate the long-term effects of IP-10 expression on the treatment of vascular restenosis.

In conclusion, the present study used RNAi to inhibit VSMC IP-10 expression and, to our knowledge, is the first to report the role of IP-10 in VSMC proliferation and restenosis after vascular angioplasty using both in vitro and in vivo experimental models. The results of this study provide a new strategy for the treatment of vascular restenosis in arteriosclerotic obliteration patients who have undergone interventional therapy.

Acknowledgments We thankfully acknowledge the financial support provided by the Key Induction Project of Science and Technology, Guangdong Province (Grants # 2010B031600055; 2006B35801010; 2005B31201001); The project was sponsored by the SRF for ROCS, SEM (Grant # 2010-609); the National 863 plans projects of China (Grant # 2007AA021904), and the Doctorate Funding Program for Higher Education, Ministry of Education, China (Grant # 20050558053).

References

1. Yajima, N., Takahashi, M., Morimoto, H., et al. (2008). Critical role of bone marrow apoptosis-associated speck-like protein, an inflammasome adaptor molecule, in neointimal formation after vascular injury in mice. *Circulation, 117*, 3079–3087.
2. Luster, A. D., Unkeless, J. C., & Ravetch, J. V. (1985). Gamma-interferon transcriptionally regulates an early-response gene containing homology to platelet proteins. *Nature, 315*, 672–676.
3. Taub, D. D., Lloyd, A. R., Conlon, K., et al. (1993). Recombinant human interferon-inducible protein 10 is a chemoattractant for human monocytes and T lymphocytes and promotes T cell adhesion to endothelial cells. *The Journal of Experimental Medicine, 177*, 1809–1814.
4. Glass, W. G., Subbarao, K., Murphy, B., & Murphy, P. M. (2004). Mechanisms of host defense following severe acute respiratory syndrome-coronavirus [SARS-CoV] pulmonary infection of mice. *The Journal of Immunology, 173*, 4030–4039.

5. Tang, N. L., Chan, P. K., Wong, C. K., et al. (2005). Early enhanced expression of interferon inducible protein-10 [CXCL-10] and other chemokines predict adverse outcome in severe acute respiratory syndrome. *Clinical Chemistry, 51*, 2333–2340.
6. Deng, G., Zhou, G., Zhang, R., et al. (2008). Regulatory polymorphisms in the promoter of CXCL10 gene and disease progression in male hepatitis B virus carriers. *Gastroenterology, 134*, 716–726.
7. Ruhwald, M., Bjerregaard-Andersen, M., Rabna, P., Kofoed, K., Eugen-Olsen, J., & Ravn, P. (2007). CXCL10/IP-10 release is induced by incubation of whole blood from tuberculosis patients with ESAT-6, CFP10 and TB7.7. *Microbes and Infection, 9*, 806–812.
8. Hanifi-Moghaddam, P., Schloot, N. C., Kappler, S., Seissler, J., & Kolb, H. (2003). An association of autoantibody status and serum cytokine levels in type 1 diabetes. *Diabetes, 52*, 1137–1142.
9. Shimada, A., Morimoto, J., Kodama, K., et al. (2001). Elevated serum IP-10 levels observed in type-1 diabetes. *Diabetes Care, 24*, 510–515.
10. Nicoletti, F., Conget, I., Di Mauro, M., et al. (2002). Serum concentrations of the interferon-gamma-inducible chemokine IP-10/CXCL10 are augmented in both newly diagnosed Type I diabetes mellitus patients and subjects at risk of developing the disease. *Diabetologia, 45*, 1107–1110.
11. Romagnani, P., Rotondi, M., Lazzeri, E., et al. (2002). Expression of IP-10/CXCL10 and MIG/CXCL9 in the thyroid and increased levels of IP-10/CXCL10 in the serum of patients with recent-onset Graves' disease. *American Journal of Pathology, 161*, 195–206.
12. Mariotti, S., del Prete, G. F., Mastromauro, C., et al. (1991). The autoimmune infiltrate of Basedow's disease: analysis of clonal level and comparison with Hashimoto's thyroiditis. *Clinical Endocrinology, 97*, 139–146.
13. Garcia-Lopez, M. A., Sancho, D., Sanchez-Madrid, F., & Marazuela, M. (2001). Thyrocytes from autoimmune thyroid disorders produce the chemokines IP-10 and Mig and attract CXCR3 + lymphocytes. *Journal of Clinical Endocrinology and Metabolism, 86*, 5008–5016.
14. Lasagni, L., Francalanci, M., Annunziato, F., et al. (2003). An alternatively spliced variant of CXCR3 mediates the inhibition of endothelial cell growth induced by IP-10, Mig, and I-TAC, and acts as functional receptor for platelet factor 4. *The Journal of Experimental Medicine, 197*, 1537–1549.
15. Lazzeri, E., & Romagnani, P. (2005). CXCR3-binding chemokines: novel multifunctional therapeutic targets. *Current Drug Targets: Immune, Endocrine & Metabolic Disorders, 5*, 109–118.
16. Melter, M., Exeni, A., Reinders, M. E., et al. (2001). Expression of the chemokine receptor CXCR3 and its ligand IP-10 during human cardiac allograft rejection. *Circulation, 104*, 2558–2564.
17. Zhao, D. X., Hu, Y. Y., Miller, G. G., Luster, A. D., Mitchell, R. N., & Libby, P. (2002). Differential expression of the IFN-gamma-inducible CXCR3-binding chemokines, IFN-inducible protein 10, monokine induced by IFN, and IFN-inducible T cell alpha chemoattractant in human cardiac allografts: association with cardiac allograft vasculopathy and acute rejection. *The Journal of Immunology, 169*, 1556–1560.
18. Fahmy, N. M., Yamani, M. H., Starling, R. C., et al. (2003). Chemokine and chemokine receptor gene expression indicates acute rejection of human cardiac transplants. *Transplantation, 75*, 72–78.
19. Kao, J., Kobashigawa, J., Fishbein, M. C., et al. (2003). Elevated serum levels of the CXCR3 chemokine ITAC are associated with the development of transplant coronary artery disease. *Circulation, 107*, 1958–1961.
20. Wang, X., Yue, T. L., Ohlstein, E. H., Sung, C. P., & Feuerstein, G. Z. (1996). Interferon-inducible protein-10 involves vascular smooth muscle cell migration, proliferation, and inflammatory response. *The Journal of Biological Chemistry, 271*, 24286–24293.
21. Mach, F., Sauty, A., & Iarossi, A. S. (1999). Differential expression of three T lymphocyte-activating CXC chemokines by human atheroma-associated cells. *The Journal of Clinical Investigation, 104*, 1041–1050.
22. Han, D. K., Haudenschild, C. C., Hong, M. K., Tinkle, B. T., Leon, M. B., & Liau, G. (1995). Evidence for apoptosis is in human atherogenesis and in a rat vascular injury model. *American Journal of Pathology, 147*, 267–278.
23. Luisis, A. J. (2000). Atherosclerosis. *Nature, 407*, 233–241.
24. Sedding, D. G., Tröbs, M., Reich, F., et al. (2009). 3-Deazaadenosine prevents smooth muscle cell proliferation and neointima formation by interfering with Ras signaling. *Circulation Research, 104*, 1192–1200.
25. Dzau, V. J., Braun-Dullaeus, R. C., & Sedding, D. G. (2002). Vascular proliferation and atherosclerosis: new perspectives and therapeutic strategies. *Nature Medicine, 8*, 1249–1256.
26. Hodges-Garcia, Y. K., Madigan, N., & Horwitz, L. D. (1998). Primary human vascular smooth muscle cell culture enhanced by human umbilical cord serum. *In Vitro Cellular & Developmental Biology Animal, 34*, 364–366.
27. Schwartz, M. A. K., Lieske, J. C., Kumar, V., Farell-Baril, G., & Miller, V. M. (2008). Human-derived nanoparticles and vascular response to injury in rabbit carotid arteries: Proof of principle. *International Journal of Nanomedicine, 3*, 243–248.
28. Rotmans, J. I., Velema, E., Verhagen, H. J., et al. (2004). Matrix metalloproteinase inhibition reduces intimal hyperplasia in a porcine arteriovenous-graft model. *Journal of Vascular Surgery, 39*, 432–439.
29. Mazzone, A., De Servi, S., Ricevuti, G., et al. (1993). Increased expression of neutrophil and monocyte adhesion molecules in unstable coronary artery disease. *Circulation, 88*, 358–363.
30. Khorsandi, M. J., Fagin, J. A., Giannella-Neto, D., Forrester, J. S., & Cercek, B. (1992). Regulation of insulin-like growth factor I and its receptor in rat aorta after balloon denudation: evidence for local bioactivity. *The Journal of Clinical Investigation, 90*, 1926–1931.
31. Linder, V., & Reidy, M. A. (1993). Expression of basic fibroblast growth factor and its receptor by smooth muscle cells and endothelium in injured rat arteries. *Circulation Research, 73*, 589–595.
32. Bornfeldt, K. E., Raines, E. W., Nakano, T., Graves, L. M., Krebs, E. G., & Ross, R. (1994). Insulin-like growth factor-I and platelet-derived growth factor-B induce directed migration of human arterial smooth muscle cells via signaling pathways that are distinct from those of proliferation. *The Journal of Clinical Investigation, 93*, 1266–1274.
33. McCaffrey, T. A. (2000). TGF-beta and TGF-beta receptor in atherosclerosis. *Cytokine Growth Factor Review, 11*, 103–114.
34. Bayes, G. A., Conover, C. A., & Schwartz, R. S. (2000). The insulin-like growth factor axis: A review of atherosclerosis and restenosis. *Circulation Research, 86*, 125–130.
35. Fire, A., Xu, S., Montgomery, M. K., Kostas, S. A., Driver, S. E., & Mello, C. C. (1998). Potent and specific genetic interference by double 2 strand RNA in *Caenorhabditis elegans*. *Nature, 391*, 744–745.
36. Kusaba, K., Kai, H., & Koga, M. (2007). Inhibition of intrinsic Interferon-γ function prevents neointima formation after balloon injury. *Hypertension, 49*, 909–915.